The Astrophysical Journal, 734:71 (10pp), 2011 June 10 doi:10.1088/0004-637X/734/1/71
© 2011. The American Astronomical Society. All rights reserved. Printed in the U.S.A.

IS THE MAGNETIC FIELD IN THE HELIOSHEATH LAMINAR OR A TURBULENT SEA OF BUBBLES?

M. Opher[1], J. F. Drake[2], M. Swisdak[3], K. M. Schoeffler[3], J. D. Richardson[4], R. B. Decker[5], and G. Toth[6]
[1] Astronomy Department, Boston University, Boston, MA, USA; mopher@bu.edu
[2] Department of Physics and the Institute for Physical Science and Technology, University of Maryland, College Park, MD, USA
[3] Institute for Research in Electronics and Applied Physics, University of Maryland, College Park, MD, USA
[4] Kavli Institute for Astrophysics and Space Research, Massachusetts Institute of Technology, Cambridge, MA, USA
[5] John Hopkins Applied Physics Laboratory, Laurel, MD, USA
[6] University of Michigan, Ann Arbor, MI, USA
Received 2010 November 1; accepted 2011 March 28; published 2011 May 25

ABSTRACT

All current global models of the heliosphere are based on the assumption that the magnetic field in the heliosheath, in the region close to the heliopause (HP), is laminar. We argue that in that region the heliospheric magnetic field is not laminar but instead consists of magnetic bubbles. We refer to it as the bubble-dominated heliosheath region. Recently, we proposed that the annihilation of the "sectored" magnetic field within the heliosheath as it is compressed on its approach to the HP produces anomalous cosmic rays and also energetic electrons. As a product of the annihilation of the sectored magnetic field, densely packed magnetic islands (which further interact to form magnetic bubbles) are produced. These magnetic islands/bubbles will be convected with ambient flows as the sector region is carried to higher latitudes filling the heliosheath. We further argue that the magnetic islands/bubbles will develop upstream within the heliosheath. As a result, the magnetic field in the heliosheath sector region will be disordered well upstream of the HP. We present a three-dimensional MHD simulation with very high numerical resolution that captures the north–south boundaries of the sector region. We show that due to the high pressure of the interstellar magnetic field a north–south asymmetry develops such that the disordered sectored region fills a large portion of the northern part of the heliosphere with a smaller extension in the southern hemisphere. We suggest that this scenario is supported by the following changes that occurred around 2008 and from 2009.16 onward: (1) the sudden decrease in the intensity of low energy electrons (0.02–1.5 MeV) detected by *Voyager 2*, (2) a sharp reduction in the intensity of fluctuations of the radial flow, and (3) the dramatic differences in intensity trends between galactic cosmic ray electrons (3.8–59 MeV) at *Voyager 1* and *2*. We argue that these observations are a consequence of *Voyager 2* leaving the sector region of disordered field during these periods and crossing into a region of unipolar laminar field.

Key words: magnetic fields – magnetic reconnection – magnetohydrodynamics (MHD) – plasmas – Sun: heliosphere

Online-only material: color figures

1. INTRODUCTION

The current understanding of the outer heliosphere has changed dramatically in the last few years due to the recent observations of *Voyager 1* and *2* (Stone et al. 2005, 2008) and *IBEX* (McComas et al. 2009). The *Voyager* data at the crossing of the termination shock (TS) revealed that the anomalous cosmic rays (ACRs) were not accelerated at the location of the spacecraft. Several scenarios have been suggested to explain these surprising observations: the ACRs could be accelerated by the TS along the flanks of the heliosphere (McComas & Schwadron 2006), in the heliosheath by compressional turbulence (Fisk & Gloeckler 2006, 2007, 2009), or by reconnection in the sectored field near the heliopause (HP; Lazarian & Opher 2009; Drake et al. 2010). Another shift in paradigm occurred when it became clear that the pickup ions carry a large portion of the plasma energy (Zank 1999; Richardson et al. 2008). Finally, the data from *IBEX* revealed a ribbon of energetic neutral atoms, suggesting that the interstellar magnetic field has a very important role in shaping the heliosphere. This result reinforces earlier *Voyager* observations: the interstellar magnetic field produces a north–south asymmetry in the location of the TS (Opher et al. 2006, 2009).

Recently, we suggested a new mechanism for the acceleration of the ACRs. We suggested that the sectored heliospheric magnetic field, which results from the flapping of the heliospheric current sheet (HCS), piles up as it approaches the HP, narrowing the current sheets that separate the sectors and triggering the onset of collisionless magnetic reconnection (Drake et al. 2010). We argued that reconnection is responsible for the acceleration of the ACRs and also energetic electrons.

We showed (Drake et al. 2010), using particle-in-cell (PIC) simulations, that the sectors break up into a bath of magnetic islands and that most of the magnetic energy goes into energetic ions, with significant but smaller amounts of energy going into electrons. The most energetic ions gain energy as they reflect from the ends of contracting magnetic islands, a first-order Fermi process. The simulations also revealed that mirror and firehose conditions play an essential role in reconnection dynamics and particle acceleration. An analytic model was constructed in which the Fermi drive, modulated by the approach to firehose marginality, is balanced by convective loss. The ACR differential energy spectrum takes the form of a power law with a spectral index slightly above 1.5.

Here we analyze the global topology of the HCS and the sector region. We argue that, within the sector region but upstream of the HP, the heliospheric magnetic field is not laminar but instead filled with nested magnetic islands. The magnetic islands/bubbles formed during reconnection of the sector region upstream of the HP are convected with the flows as the sector boundary is carried to higher latitudes, filling the heliosheath upstream of the HP.

We argue that due to the increased pressure of the interstellar magnetic field (Opher et al. 2006, 2007) the sector region and embedded islands are carried mostly to the northern hemisphere. We therefore predict an asymmetry of the magnetic structure between the northern and southern hemispheres and between the heliosheath sectored region and the field outside of it. Therefore, we predict that the northern hemisphere will be predominantly a disordered field filled with magnetic islands and not a laminar field.

We further argue that the magnetic islands might develop upstream (but still within the heliosheath) where collisionless reconnection is unfavorable—large perturbations of the sector structure near the HP might cause compressions of the current sheet upstream, triggering reconnection. As a result, the magnetic field in the heliosheath sector region will be disordered well upstream of the HP. If this hypothesis is correct, the *Voyager* satellites may already have crossed into a region of disordered field consisting of nested magnetic islands. We present data from reconnection simulations of a sectored magnetic field, using a PIC code that, surprisingly, exhibits characteristics similar to the *Voyager* data: the magnetic field exhibits reversals, but with a more erratic spacing than the initial state, and reconnection of the nested islands is suppressed due to the approach to the firehose marginal stability condition so plasma flows are irregular and only occasionally exhibit traditional reconnection signatures. We refer to the late-time non-reconnecting magnetic islands as "bubbles" since in cross section they more closely resemble a nested volume of soap bubbles than a system of reconnecting islands.

Energetic electrons are especially sensitive to the large-scale magnetic structure of the heliosheath because of their high velocity. The presence of magnetic islands/bubbles in the heliosheath sector region will change the electron transport. Specifically, a disordered heliospheric magnetic field near the HP acts as the window through which galactic cosmic ray (GCR) electrons traveling along the interstellar magnetic fields can enter and percolate through the heliosphere. Magnetic islands/bubbles will act as local traps for these energetic electrons. Since lower energy electrons are produced during reconnection in the sectored field in the same region, these two classes of electrons should display similar modulation characteristics. Therefore, we argue that there should be a north–south asymmetry between the electron intensities at *Voyager 1* and *2*, and between the intensities measured while the spacecrafts are within the bubble-dominated region and outside of it.

This prediction will change our view of the heliosphere since all the current global models (e.g., Opher et al. 2006, 2009; Heerikhuisen et al. 2010; Pogorelov et al. 2007; Ratkiewicz & Grygorczuk 2008) are based on the presumption that the magnetic field is laminar in the outer heliosheath close to the HP and in the heliosheath sector region. More recently, Czechowski et al. (2010) analyzed the behavior of the HCS in a kinematic model. They suggested that close to the HP mixed polarities could reconnect making the field random.

We present *Voyager 1* and *2* data that support this disordered field hypothesis. *Voyager 1* and *2* are moving through the sectored region and are near the boundary between the sectored and non-sectored region, and have therefore sampled both regions.

The structure of this article is the following: in the next section we show the global behavior of a modeled sector region based on an MHD description. This will set the context for the *Voyager* trajectories compared with the sector region. We then present *Voyager 1* and *2* observations that support our proposed scenario. We then present the results of PIC simulations of the sector region and discuss the structure of the resulting nested magnetic islands/bubbles and plasma flows. Finally, we discuss the implications of our predictions for understanding current measurements by *Voyager 2*, and our global understanding of the heliosheath, the sector region, and HP.

2. GLOBAL BEHAVIOR OF THE SECTOR BOUNDARY

Because of the tilt between the solar rotation and magnetic axis, the actual HCS oscillates up and down, producing a magnetic field with a "ballerina skirt" shape. The drop of the solar wind speed beyond the TS causes the sectors to compress. This behavior was demonstrated in MHD simulations in Drake et al. (2010) and with greater resolution by Borovikov et al. (2011). At the current stage in the solar cycle, the limits of the sector boundary are approximately $\pm 30^\circ$, close to the latitudes of *Voyager 1* and *2*.

We have carried out simulations with a sector region with a latitudinal width of 60°. We used the three-dimensional MHD multifluid model described in Opher et al. (2009). This model is based on BATS-R-US (for a more recent description see Toth et al. 2011). Our model has five fluids (similar to Alexashov & Izmodenov 2005 and Zank et al. 1996). In this approach there are four populations of neutral H atoms, one for every region in the interaction between the solar wind and the interstellar wind. Population 4 represents the H atoms of interstellar origin. Population 1 represents the H atoms that exist in the region between the bow shock and the HP. Populations 3 and 2 represent the H atoms in the supersonic solar wind and in the compressed region between the TS and the HP, respectively. All four H populations are described by separate systems of the Euler equations with the corresponding source terms. Each population is created in its respective region but is free to move between the different regions as the simulation evolves. The ionized component interacts with the H neutrals via charge exchange (for more details see Opher et al. 2009). The parameters for the density, velocity, and temperature of the ions and neutrals in the interstellar medium reflect the best observational values. The parameters for the inner boundary (located at 30 AU) were chosen to match those used by Izmodenov (2009): proton density $n = 8.74 \times 10^{-3}\,\mathrm{cm}^{-3}$, temperature $T = 1.087 \times 10^5$ K, speed $v = 417\,\mathrm{km\,s}^{-1}$, and a Parker spiral magnetic field with strength $B = 7.17 \times 10^{-3}$ nT at the equator. The outer boundary conditions are $n = 0.06\,\mathrm{cm}^{-3}$, velocity equal to $26.3\,\mathrm{km\,s}^{-1}$, and $T = 6519$ K. The neutral hydrogen in the local interstellar medium is assumed to have $n = 0.18\,\mathrm{cm}^{-3}$ and the same velocity and temperature as the ionized local interstellar medium.

The interstellar magnetic field intensity B_{ISM} taken was $4.4\,\mu$G and the orientation was such that the angle between the interstellar velocity and the magnetic field was 20°, and the angle between the plane containing the interstellar velocity and the magnetic field and the solar equator was 60°. This orientation and intensity produced the asymmetries in the TS locations as measured by the *Voyager* satellites (Opher et al. 2009). Matching the heliosheath flows measured by *Voyager 2* requires slightly different values (Opher et al. 2009). This chosen orientation is close to the one inferred from *IBEX* (McComas et al. 2009) and the ones currently used based on hydrogen deflection arguments (Pogorelov et al. 2008).

We used fixed inner boundary conditions for the ion and neutral fluids. The outer boundaries were all outflows with the

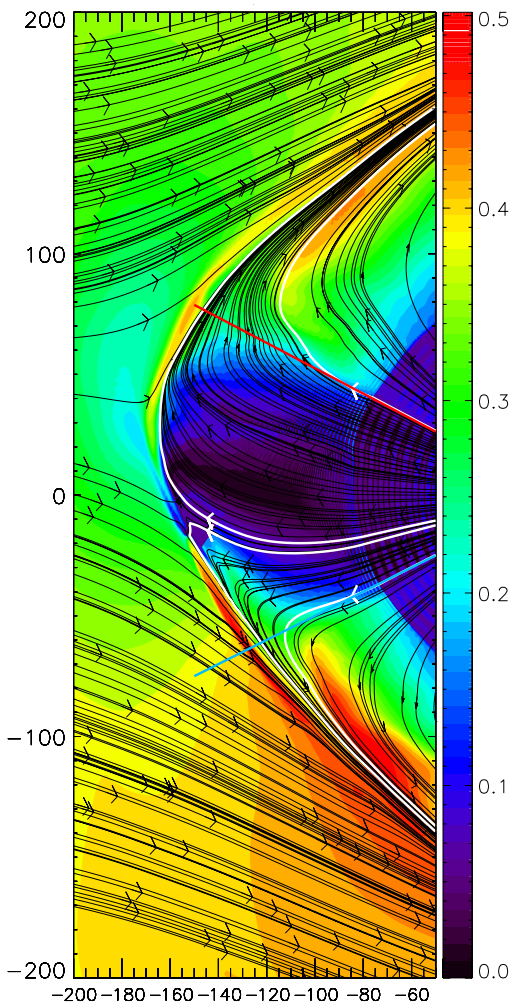

Figure 1. Meridional cut from a three-dimensional MHD simulation showing the magnitude of the magnetic field (nT). The sector region of width of 60° is the blue–black region. The flow streamlines are shown in black. The boundary of the sector region is shown in the white streamlines. The *Voyager 1* trajectory is 30° above the solar equator and that of *Voyager 2* is 29.°8 below the solar equator and are shown, respectively, in the red and blue lines.

(A color version of this figure is available in the online journal.)

exception of the $-x$ boundary, where the inflow conditions were imposed for the ionized fluids and the population of neutrals coming from the interstellar medium (Population 4). The outer boundaries of the grid are set at -1000 AU and 1000 AU in the x-, y-, and z-directions, respectively. The description of the coordinate system is given in Opher et al. (2009).

To capture the sector boundary in the heliosheath, adaptive mesh refinement was used. Several refinements were done throughout the computational run. The final computational cells range from 0.03 AU to 31.25 AU. The block used had $8 \times 8 \times 8$ cells (see Toth et al. 2011). The total number of cells was 1.4×10^9. The simulation presented here took 230,000 time steps on approximately 2000 CPUs. More details of this simulation and the steps involved are given in M. Opher et al. (2011, in preparation).

Figure 1 shows the distribution of the magnitude of the magnetic field in the meridional plane (x–z plane). The sector spacing decreases downstream of the TS and further decreases on the approach to the HP. The approximate trajectories of

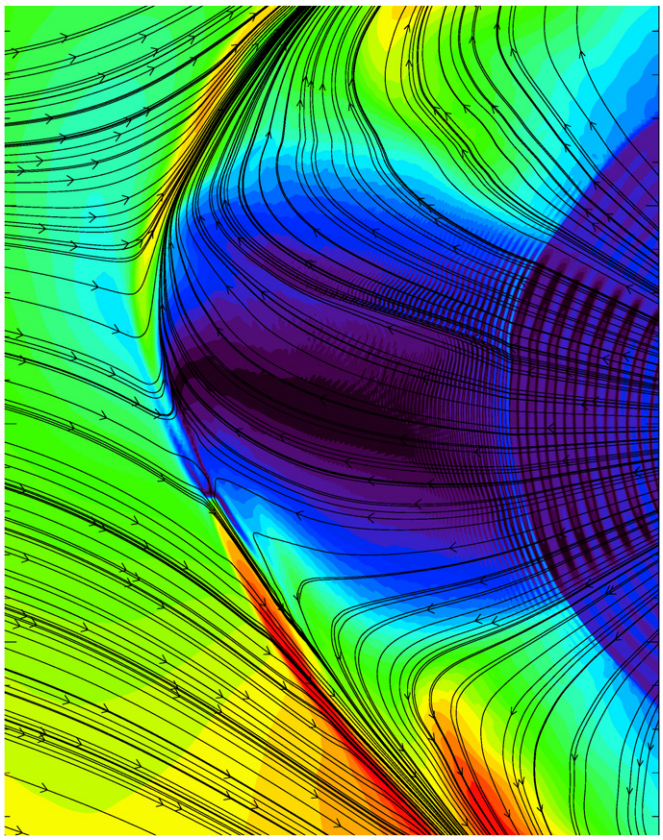

Figure 2. Blowup of the sector region of Figure 1.

(A color version of this figure is available in the online journal.)

Voyager 1 and *2* are indicated with red and blue lines, respectively. Figure 2 shows a blowup of the same meridional cut.

There is an asymmetry of the heliosphere due to the interstellar magnetic field. The inclination of the interstellar magnetic field compresses the southern hemisphere, pushing the HP and the TS in this region closer to the Sun (Opher et al. 2006, 2007, 2009). The effect of the difference in pressure between the north and south is to deflect the sector boundary to the north. Figures 1 and 2 show this effect.

We are able to resolve the alternating sectors out to the middle of the heliosheath. The sector structure is compressed downstream of the TS (the sector spacing decreases from 4.7 AU to 1.9 AU) and the spacing of the sectors continuously decreases further into the heliosheath as the radial plasma velocity decreases. Deep into the heliosheath, resolutions finer than 0.03 AU are needed. In any case, the sectors close to the HP are expected to reconnect and possibly trigger reconnection further upstream. The decrease in the spacing of the sectors is seen in Figures 2 and 3. Figure 3 presents a zoom of the sectors between the region just upstream of the TS into the heliosheath. The decrease in the spacing of the sectors can be seen as the solar wind crosses the TS. The loss of resolution deep in the heliosheath can be seen as well.

In the heliosheath, the heliospheric magnetic field, to lowest order, simply adds to the dominant thermal pressure so the sector structure is not expected to alter the large-scale plasma flow pattern. Thus, we can simply follow the flow streamlines to determine what fraction of the sector region will be carried to the northern hemisphere even though the resolution is insufficient to define the sectors. This same procedure was recently followed by Czechowski et al. (2010). The white

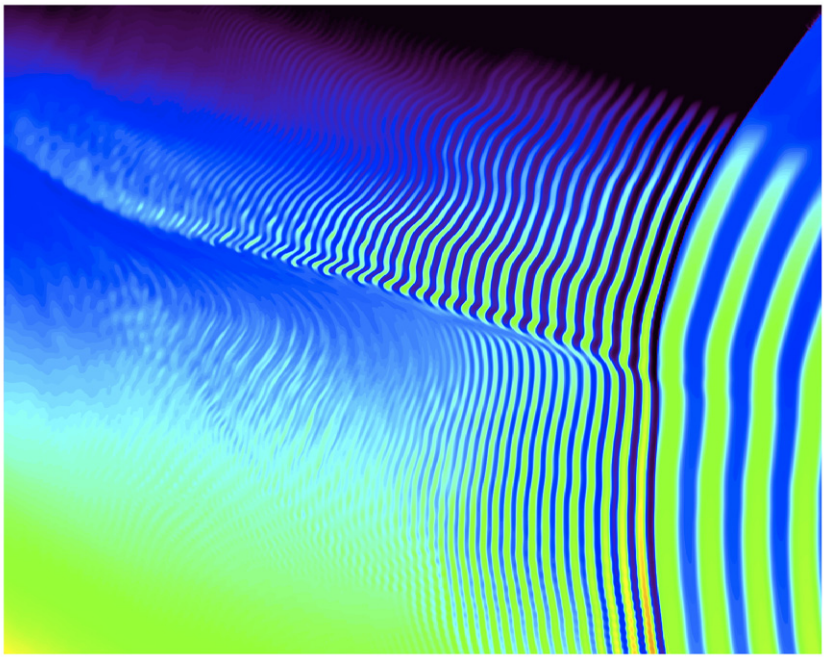

Figure 3. Zoom of the sectors between the regions just upstream of the termination shock into the heliosheath. The decrease in the spacing of the sectors can be seen as the solar wind crosses the termination shock. The loss of resolution deep in the heliosheath can be seen as well.
(A color version of this figure is available in the online journal.)

streamlines in Figure 1 show the boundary of the sector region. With increased resolution and a longer simulation time we expect the sector region to fill the domain bounded by the white streamlines. We can see that the northern sector region is much thicker than the sector region carried to the south. The thickening of the northern sector region results from the increased pressure of the interstellar magnetic field in the south, which diverts the overall heliosheath flow to the north. Thus, it is evident from Figure 1 that a simple straight-line extrapolation of the latitudinal extent of the sector region fails deep into the heliosheath, especially in the north. This could explain why early in 2009 *Voyager 1* seemed to be in a unipolar region, while later in 2009 *Voyager 1* reentered the sector region (Burlaga & Ness 2010).

As mentioned earlier, we predict (Drake et al. 2010) that in the heliosheath, near the HP, the magnetic fields in the sector region will reconnect, forming nested magnetic islands. We expect the reconnection to be most robust close to the HP. On the other hand, the perturbations of the sector structure due to reconnection near the HP will cause compressions of the current sheets upstream, possibly triggering reconnection there. The heliosheath flows will carry the magnetic islands/bubbles within the sector region to higher latitudes. Because the dominant heliosheath flow is northward, we therefore predict an asymmetry of the magnetic structure between the northern and southern hemispheres.

3. OBSERVATIONS OF *VOYAGER 1* AND *2* THAT SUPPORT OUR SCENARIO

We present *Voyager 1* and *2* data that support our disordered field scenario in Figures 4–6. The shaded gray regions are the unipolar regions and the unshaded regions (beyond 2008) correspond to the sector region (the proposed bubble region). Figure 4 shows daily averages of the intensity of the magnetic field. In the period of 2008–2008.2 and from 2009.15 on (shaded areas), *Voyager 2* had a positive polarity ($\lambda = 270^{\circ}$) with only infrequent excursions to negative polarities. In the time period of 2009.15 on, the field was 90% in the positive polarity with 10% in the negative polarity. Figure 5 shows the daily average of the intensity of electrons from 0.022 to 0.035 MeV, 0.035 to 0.061 MeV, and 0.35 to 1.5 MeV. Around the period of 2008–2008.2 and from 2009.15 on (shaded areas), there was a drop in the intensity of electrons as measured by *Voyager 2*. The drop was especially dramatic after 2009.15. Figure 6 shows 0.2 year averages and standard deviations of the radial flows. The measured unipolar regions (between 2008–2008.2 and 2009.15–2009.41) are shaded gray and the conjectured unipolar region (after 2009.41) is shaded light gray. We can see that there is a large increase in the intensity of fluctuations in the sector region (non-shaded) as compared with the unipolar regions (shaded). These observations will be discussed more fully after we present the results of the PIC simulations and associated discussion.

4. DISORDERED MAGNETIC FIELD IN THE HELIOSHEATH SECTOR REGION

We also present results from kinetic simulations carried out with the PIC code p3d. The algorithm used is described in detail in Zeiler et al. (2002). Here we present the results of simulations reported earlier in Drake et al. (2010). The initial state had eight current layers that produced a magnetic field, B_Y, with periodic reversals. Reconnection spontaneously developed and was followed in time. Detailed parameters of these runs were presented in Drake et al. (2010).

As discussed in Drake et al. (2010), we argued that the compression of the sectors on their approach to the HP would narrow the HCS sufficiently enough to trigger reconnection of the sector field. In Figures 7(a) and 8(a), we show the modulus of the magnetic field B early ($\Omega_p t = 100$) and later ($\Omega_p t = 150$), with Ω_p being the proton cyclotron frequency, to illustrate the

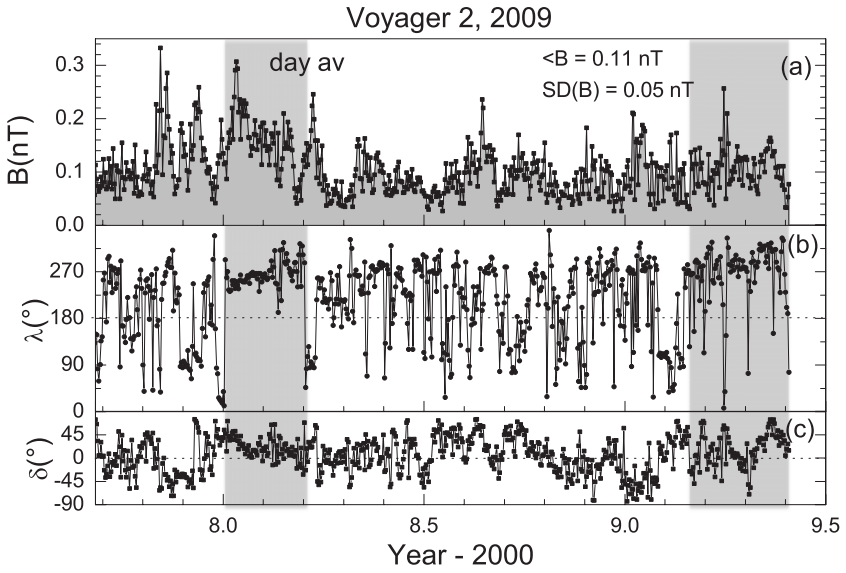

Figure 4. Daily averages of the (a) magnetic strength B, (b) azimuthal angle λ, and (c) elevation angle δ measured by *Voyager 2*. The azimuthal angle λ and the elevation angle δ of B are defined as $\lambda = \tan^{-1}(B_Y/B_X)$ and $\delta = \sin^{-1}(B_z/B)$, where B_X, B_Y, and B_Z are the magnetic field components in the heliographic coordinate system. The unipolar periods between 2008–2008.2 and from 2009.15 on are shaded in gray. The non-shaded regions correspond to the sector region (proposed "bubble" region) (courtesy of L. Burlaga; Burlaga et al. 2010; reproduced/modified by permission of American Geophysical Union).

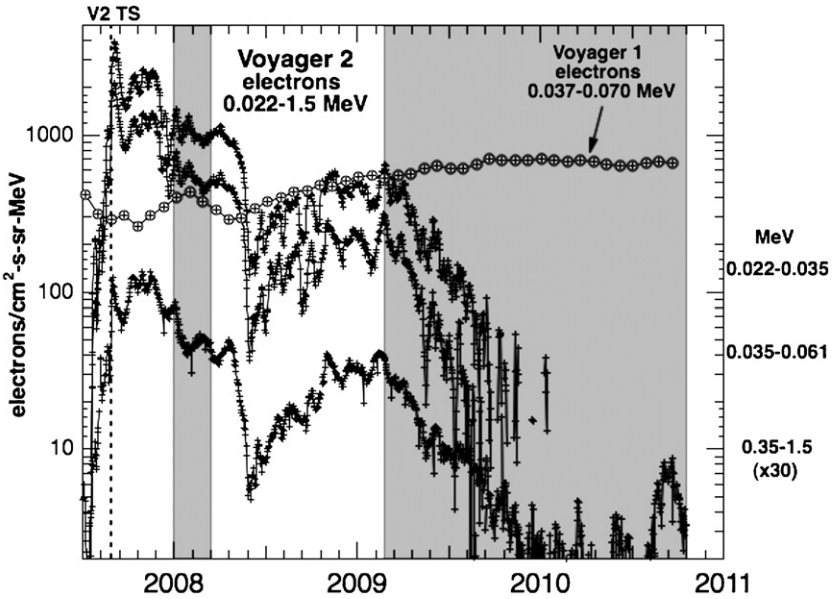

Figure 5. Daily average of the intensity of electrons from 0.022 to 0.035 MeV, 0.035 to 0.061 MeV, and 0.35 to 1.5 MeV. In the unipolar periods around 2008–2008.2 and from 2009.15 on (shaded areas), there is a drop in the intensity of electrons as measured by *Voyager 2*. The drop was especially dramatic after 2009.15. The non-shaded regions, after 2008, correspond to the sector region (the proposed "bubble" region).

magnetic topology and the variability of B as reconnection proceeds. In these simulations, y and x correspond to the heliospheric azimuthal and radial directions and d_p is the proton inertial length. The ion flows in the azimuthal direction, v_{py}, are shown at three times in Figure 9, the first two plots corresponding to Figures 7 and 8 and the third to $\Omega_p t = 200$. Early in time, the driven outflows from reconnection are evident, while later in time, especially by $\Omega_p t = 200$, the flows are erratic and do not exhibit classical reconnection signatures. In Figure 10 are the three components of the ion velocity—tangential (dotted), radial (solid), and normal (dashed)—along a cut at $y = 240 d_p$ at $\Omega_p t = 200$. This is the same time as the two-dimensional plot of v_y shown in Figure 9(c). The absence of reconnection at a later time is not because the magnetic free energy has been completely depleted. Cuts through the simulation along the radial direction (at $y = 240 d_p$) in Figures 7(b) and 8(b) show B and the heliospheric elevation angle (defined as the angle between the magnetic field and the radial direction). Even late in time substantial magnetic energy remains. Further, a casual glance at the behavior of λ might suggest that the sectors are still intact, although with a more irregular spacing than before. These "sectors," however, correspond to magnetic islands, whose size is comparable to the original sector spacing. The absence of ongoing reconnection is a consequence of firehose stability: the interior of these islands is at the marginal firehose condition $(1 - 4\pi(P_{\|} - P_{\perp})/B^2 = 0)$, where $P_{\|}$ and $P_{\perp}$ represent the parallel and perpendicular components of the pressure, where the magnetic tension that drives reconnection goes to zero

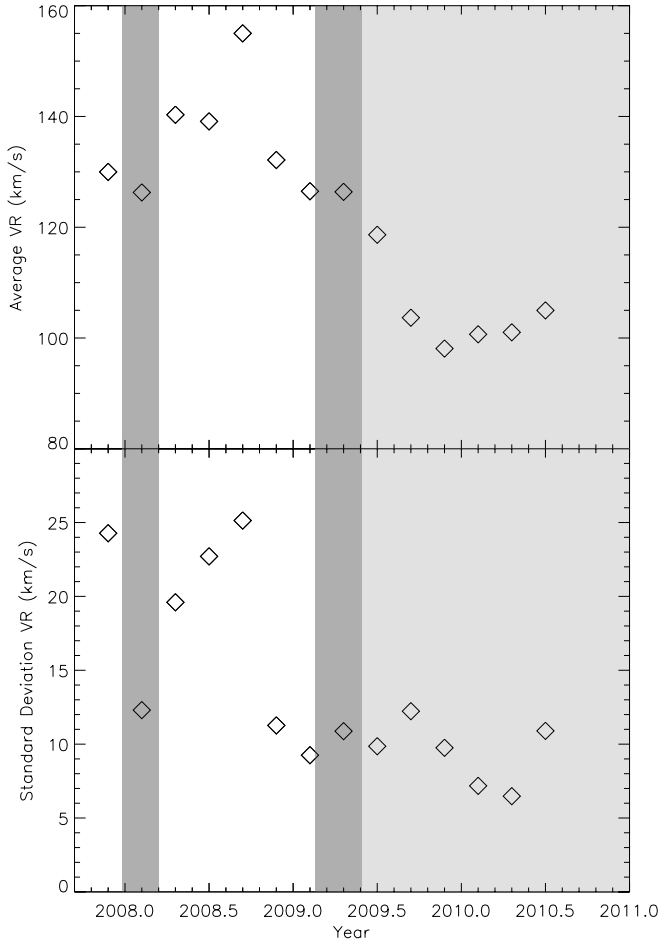

Figure 6. (a) 0.2 year averages of the radial flows and (b) standard deviations of the radial flows as measured by *Voyager 2* from 2008.7 to 2010.5. The measured unipolar regions (between 2008–2008.2 and 2009.15–2009.41) are shaded gray and the conjectured unipolar region (after 2009.41) is shaded light gray. The non-shaded regions correspond to the sector region (proposed "bubble" region).

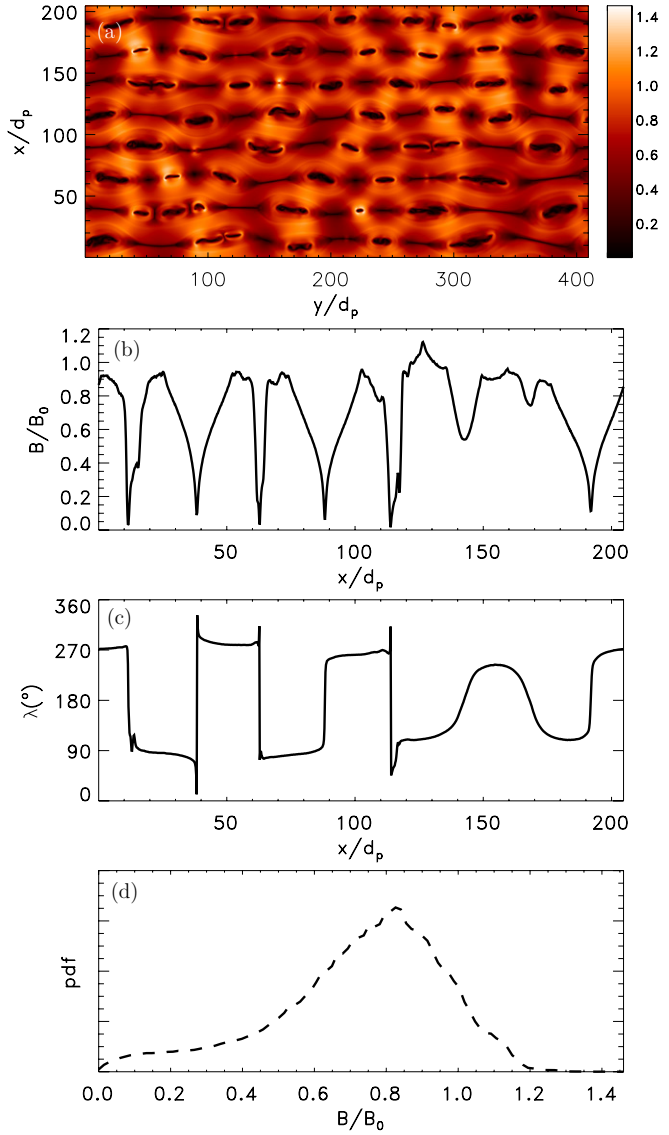

Figure 7. Magnetic field structure at $\Omega_p t = 100$ from the PIC simulation described in Drake et al. (2010) where the initial state had $\beta = 0.2$. Panel (a) shows the magnitude of the magnetic field B during reconnection of the sectors, (b) the magnetic field intensity in a cut along $y = 240 d_p$, (c) angle λ along $y = 240 d_p$, and (d) the distribution of the magnetic field from the simulation (dashed line).

(A color version of this figure is available in the online journal.)

(Drake et al. 2006, 2010). Thus, the predicted late-time structure of the sector field consists of nested islands with irregular spacing, but with scale sizes comparable to the original sector spacing. The remnant flows are erratic and do not exhibit the classic reconnection signatures.

A fundamental question is therefore how far upstream from the HP the nested-island, disordered field extends. While we argued in Drake et al. (2010) that reconnection would only onset close to the HP where the thickness of the HCS could approach d_p, it is possible the reconnection near the HP could spread upstream as the jostling of reconnected islands propagates upstream.

A theoretical exploration of the upstream spread of reconnection in the sectored field is beyond the scope of the present paper. We argue, however, that the *Voyager 2* data presented in Section 3 provide substantial support for the idea that the sector field encountered by *Voyager 2* has already undergone reconnection and that the measured magnetic field is in the disordered state shown in Figure 8. The irregular "sector" structure seen in the data corresponds to the irregular magnetic island spacing of Figure 8. The near absence of classic reconnection signatures in the plasma flows in the *Voyager* data is consistent with their absence in the simulation data. Moreover, at least one reconnection site has been identified in the *Voyager 2* data (Burlaga & Ness 2009; the presence of *D-sheets* was interpreted as evidence for by reconnection Burlaga & Ness 1968) that implies the existence of the occasional reconnection event at a later time when the magnetic islands merge. Further, the enhanced amplitude of fluctuations in the radial flow data in the sector region compared to unipolar regions (Figure 6) suggests reconnection as the source of the irregular flows. No other driver for these flows, which appear only in the sector region, has been proposed.

The distribution of the azimuthal angle λ is another indicator of a bubble stage. We plot in Figure 11 the distribution of λ for two periods: (a) days 0–65 of 2001 where *Voyager 2* was immersed in a sector region upstream of the TS (Burlaga et al. 2003) and (b) between 2008.3 and 2009 downstream of the TS. We did not include data where the magnitude of the magnetic field was <0.05 nT because, as noted by Burlaga et al. (2010), this is approaching the resolution limit of the magnetometer.

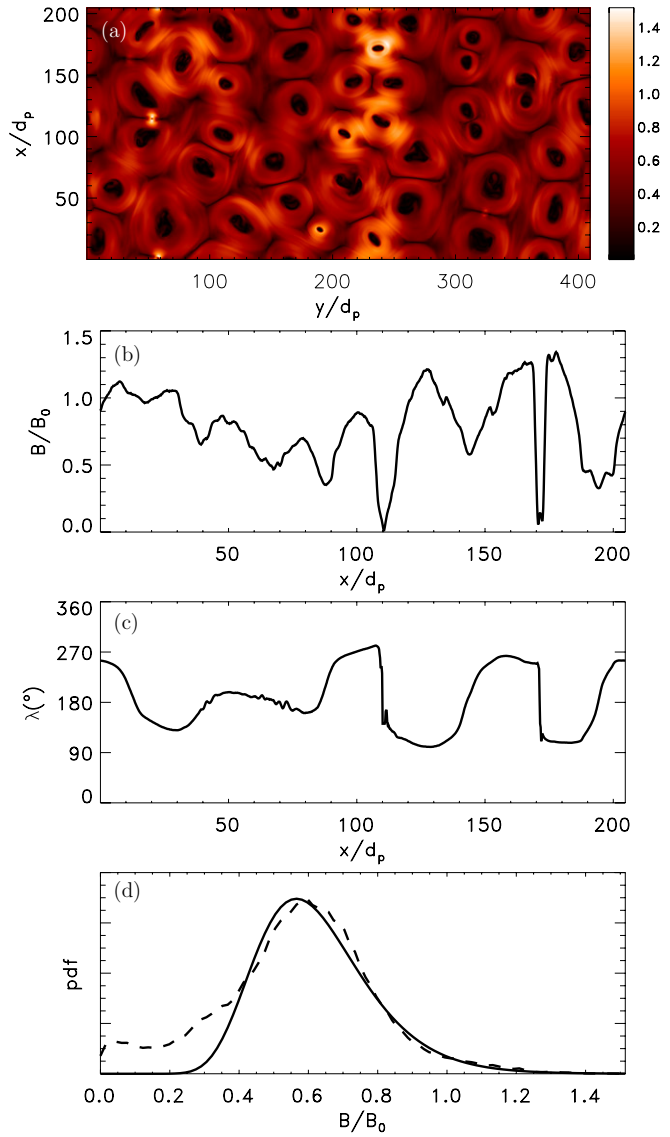

Figure 8. Same as Figure 7 but at $\Omega_p t = 150$. The solid line in (d) is a log-normal distribution.

(A color version of this figure is available in the online journal.)

Period (b) is representative of a period where we argue that the sector region is in a bubble state. We expect that, similar to Figure 8, λ would be less organized than in the regular sector region (period (a)). This can be seen in Figure 11. The distribution is broader in period (b) than in period (a).

A final piece of evidence in favor of a disordered magnetic field concerns the probability distribution of the magnetic field strength measured by *Voyager 2*. In the sector region the probability distribution has been empirically found to be log-normal, while it appears Gaussian in unipolar regions. The distribution of B from the PIC simulations is shown in Figures 7(d) and 8(d). Early in time, the distribution does not match an obvious form. However, later in time the distribution of B from the simulation (dashed line) matches a log-normal distribution (solid line) surprisingly well at large B. The match is not good at small B. The discrepancy at small B may be because the initial magnetic distribution consisted of simple antiparallel fields, while in reality the field rotates in the reversal region so there are no regions of zero field (Smith 2001). In the simulations the tails of high magnetic fields arise as the magnetic bubbles,

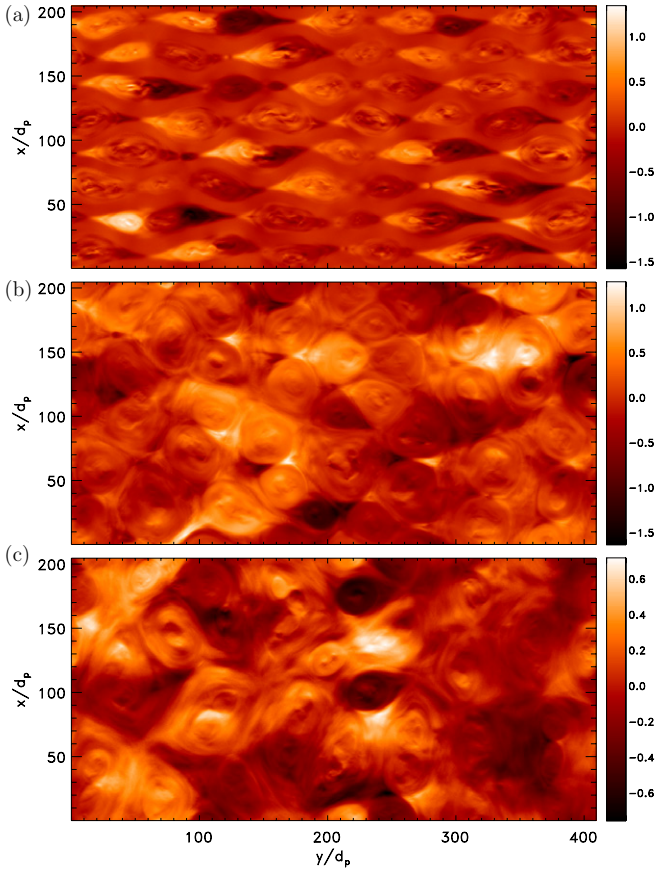

Figure 9. Flows of the protons in the azimuthal direction (v_{py} at three times ($\Omega_p t = 100, 150, 200$)).

(A color version of this figure is available in the online journal.)

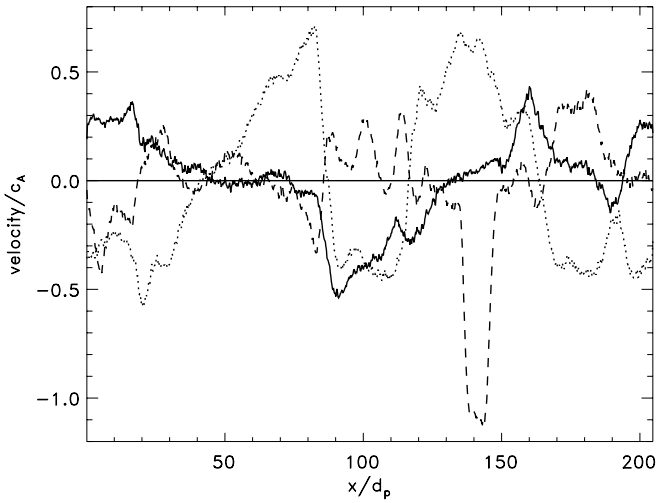

Figure 10. Three components of the ion velocity, tangential (y; dotted), radial (x; solid), and normal (z; dashed) along a cut at $y = 240 d_p$ at a time of $\Omega_p t = 200$. This is the same time as the two-dimensional plot of v_y shown in Figure 9(c).

which exhibit substantial motion even after reconnection has largely ended (see Figures 9(c) and 10), bounce off one another, compressing magnetic flux lying between the colliding bubbles (white regions of Figure 8(a)). This behavior can be most clearly seen in movies of the two-dimensional evolution of B (not shown). This behavior does not take place during the reconnection phase of the initial current sheets (Figures 7(b) and (c)).

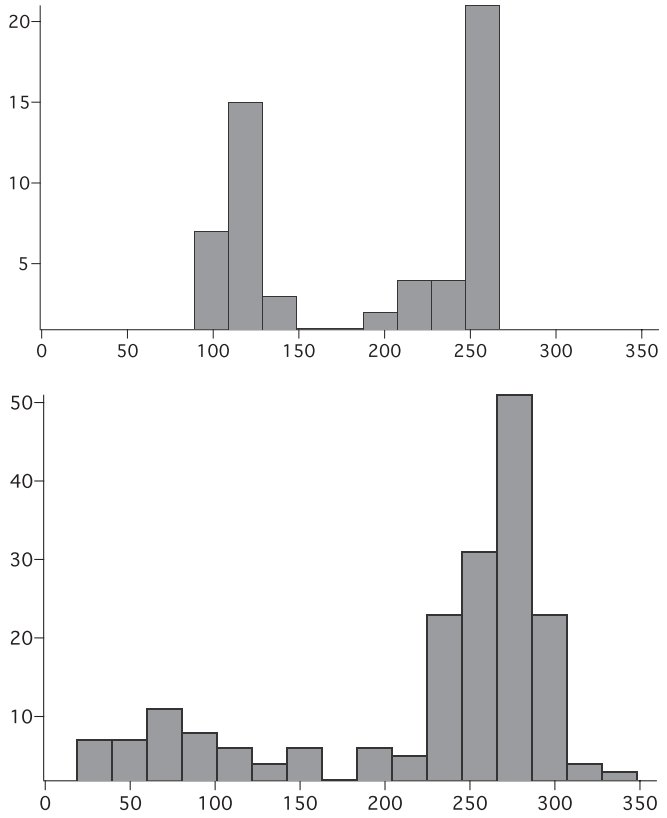

Figure 11. Distribution of the azimuthal angle λ in a normal sector (a) and a bubble period (b). Days 0–65 of 2001 where *Voyager 2* was immersed in a sector region (a) (Burlaga et al. 2003) and between 2008.3 and 2009(b). We did not include data where the magnitude of the magnetic field was <0.05 nT because this is approaching the resolution limit of the magnetometer.

The heliosheath magnetic field data from *Voyager 1* also support the idea that the heliosheath field in the sector region has already reconnected. During the 2007.4–2008.2 time period (Burlaga et al. 2009), the spacecraft was in a region of negative polarity, indicating that it was possible that the spacecraft was outside of the sector region in the region of northern polarity. During this time the fluctuations in magnetic field strength dropped significantly compared to time intervals when the spacecraft was in the sector region. The higher level of fluctuations in the sector region is consistent with that expected from the nested-bubble state after reconnection of the sector field (Figure 9). Finally, on day 254 of 2009 (Burlaga & Ness 2010) *Voyager 1* entered into a region of positive polarity and remained there through the remainder of 2009. Presumably, the spacecraft was in the sector region during this period, but due to the low radial flow in the heliosheath remained in a single sector. During this time period the magnetic field data exhibited a high level of fluctuation: the magnetic field statistics during all of 2009 exhibited a log-normal distribution (with a pronounced tail of high magnetic field events), but during the period of days 1–254 exhibited a more Gaussian distribution. Again, these observations suggest that the sector region in the vicinity of *Voyager 1* is in a disordered state.

An important question is why, even when leaving the sector region for brief periods (e.g., during 2006.2), did the intensity of the low energy electrons not drop at *Voyager 1* (Figure 5)? One possibility is that this is because of the much thicker sector region in the northern hemisphere compared with that in the southern hemisphere (Figure 1): the thicker sector region in the

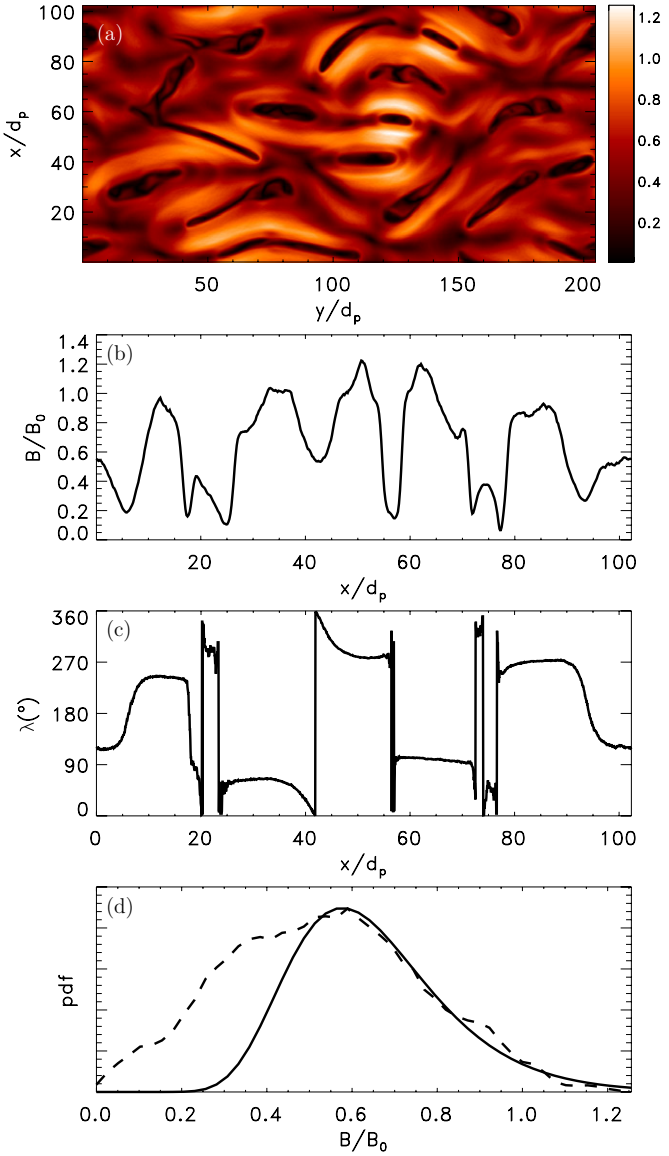

Figure 12. Same as Figure 8 for a case with $\beta = 4.8$ in the initial state. Panels (b) and (c) show cuts along x for $y = 127.5d_p$. The solid line in (d) is a log-normal distribution.

(A color version of this figure is available in the online journal.)

north is a much stronger source of energetic electrons than that in the south and is able to maintain a high flux of the electrons even in the unipolar region. A second possibility, based on the electron data, is that *Voyager* never left the sector region and due to the low radial flow was surfing the sectors. Discriminating between these two hypotheses will require a careful modeling effort taking into account the disordered field in the outer heliosphere.

The evolution of the reconnection in a sector field depends strongly on the β = thermal pressure/magnetic pressure of the initial plasma. At higher values of β reconnection is dominated by longer wavelength modes and island contraction quickly causes the plasma within islands to hit the marginal firehose condition, which suppresses reconnection (K. Schoeffler et al. 2011, in preparation). As a result, the islands at a late time in the high β case remain elongated rather than nearly round as in the case of low β. This difference can be seen by comparing the geometry of islands at a late time for the $\beta = 0.2$ initial state (Figure 8(a)) versus that for $\beta = 4.8$ (Figure 12(a)). The high

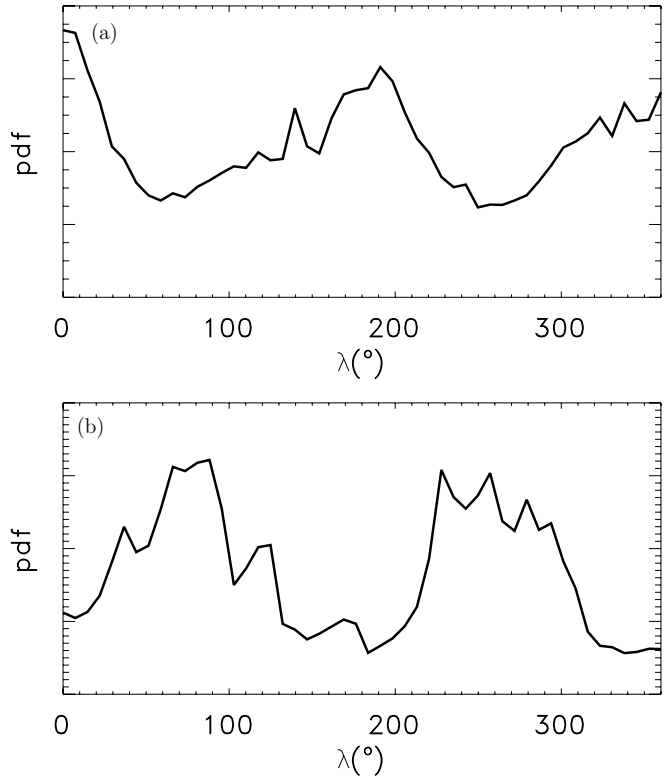

Figure 13. Distribution of λ over the entire simulation domain for initial conditions with (a) $\beta = 0.2$ and (b) $\beta = 4.8$.

β case continues to exhibit regions of intense magnetic field (Figures 12(a) and (b)) and the distribution of B again takes the form of a log-normal distribution (Figure 12(d)).

The round versus elongated structure of bubbles at a later time has a dramatic impact on the distribution of λ and therefore offers an important clue about the late-time magnetic structure of the heliosheath. A cut of λ for $\beta = 4.8$ is shown in Figure 12(c). The differences in the λ distributions for the low and high β can be seen most clearly in the distribution of λ averaged over the entire computational domain (Figure 13). Shown in Figure 13(a) are the data for the $\beta = 0.2$ initial state and in Figure 13(b) are those for the $\beta = 4.8$ initial state. The distribution of λ for the $\beta = 0.2$ case has peaks at $0°/360°$ and $180°$, while for the $\beta = 4.8$ case it peaks around $90°$ and $270°$ but with a broad distribution. The distribution of λ at $\beta = 4.8$ is similar to the *Voyager 2* data in the hypothesized bubble region. The value of β in the heliosheath is unknown, but there are indications that it is high due to the contributions from the suprathermal population of pickup ions.

5. DISCUSSION

Our prediction is that there will be an asymmetry between the northern and southern hemispheres with respect to the structure of the heliospheric magnetic field close to the HP. In the northern hemisphere, and to a lesser extent in the southern hemisphere, there will be a disordered field resulting from reconnection of the sectors. Additionally, we predict that upstream of the HP but within the sector region the magnetic field will be disordered as well (see Figure 14). The present PIC simulations are two-dimensional in the plane of the reversals of the magnetic field. This plane corresponds to the azimuthal plane in three dimensions, that is, in the x–y plane in Figure 14. The structure

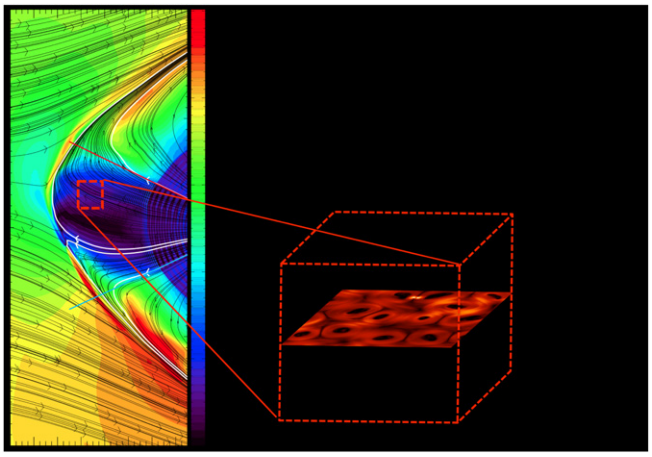

Figure 14. Representation of what we expect the outer heliosphere to be a bath of bubbles. The plane from the MHD simulation is a meridional plane, an x–z plane. The PIC simulation was done in the azimuthal plane, the x–y plane.
(A color version of this figure is available in the online journal.)

and dynamics of the bubbles in three dimensions are issues that will be explored in a future work.

Energetic electrons are especially sensitive to the topological structure of magnetic fields. The presence of magnetic islands/bubbles can significantly impact the transport of energetic electrons (and ions) in the heliosheath compared with that in a laminar region. While in a laminar field, the transport is dominated by field-aligned motion in longitude; magnetic islands/bubbles in the x–y plane strongly inhibit such motion. In the disordered field in the northern hemisphere (and the part that was carried to the south), convective transport may compete with field-aligned streaming in controlling the spatial distribution of electrons (and ACRs).

We predict that the electrons and ions accelerated in the heliosheath close to the HP will have much different transport characteristics in a disordered sector field in comparison with the laminar field in the unipolar region. The electrons (and ions) will be locally trapped on magnetic islands in a reconnected sector region and will make their way through the heliosheath in a complex diffusion process: magnetic islands will act as local storage vessels for energetic particles. Once the electrons are in a region of ordered field they will rapidly escape. Upstream of the TS and at latitudes above and below the sector boundary the field retains its nominal laminar Parker structure. Once the electrons access the Parker field they rapidly escape toward the inner heliosphere. The TS and the sector boundaries therefore act as sinks for energetic electrons. We would expect the energetic electron population in the heliosheath to be much larger than that upstream of the TS, which is what is observed.

The observations support this scenario. From Figure 4 we argue that *Voyager 2* crossed into a region of unipolar field in the period of 2009.15 onward (90% of the time the field was negative from 2009.15 to 2009.4). In the period between 2008 and 2008.2 *Voyager 2* also crossed into a unipolar region. These two periods (shaded areas) correspond to a drop in the intensity of electrons in the energy range (0.02–1.5 MeV) measured by *Voyager 2*, while the energetic electrons at *Voyager 1* remained at the same level or even increased (Figure 5). These two periods also coincide with the periods when the fluctuations of the radial flows as measured by *Voyager 2* were low, as seen in Figure 6. This is evidence that in these periods *Voyager 2* left a region of disordered field where electrons were trapped within

magnetic islands. The electrons then accessed the laminar Parker field and rapidly escaped. We further expect some anisotropy of electrons before and after mid-2009.15 in the Low Energy Charged Particle Experiment.

The disordered heliospheric magnetic field near the HP will affect the entrance and modulation of GCR electrons, making the northern hemisphere more "transparent." The GCR electrons traveling along the interstellar magnetic fields can enter and percolate through the heliosphere. The ones entering the northern hemisphere will travel through the disordered field of the sector region, while those in the southern hemisphere will access a laminar field more quickly and escape. We therefore expect a north–south asymmetry in the intensity and modulation of the GCR electrons.

This picture is in agreement with the observations of F. McDonald (2010, private communication), which exhibit a dramatic asymmetry between *Voyager 1* and *2* in the intensity of GCR electrons with energies of 3.8–59 MeV. The intensities at *Voyager 1* continue to rise, while those at *Voyager 2* reached a plateau well below that of *Voyager 1*.

As described above, our scenario predicts that the transport of particles will be different inside and outside the sector region. In particular, it predicts that independent of the solar cycle there should be an increased source of GCRs and energetic electrons at lower latitudes. The energetic electrons and GCR entering the heliosphere will percolate through the bubbles until leaving the sector region and quickly migrating into the inner heliosphere.

This scenario also will affect our understanding of reconnection at the HP, where we argued that the most favorable location for reconnection was where the interstellar magnetic field was antiparallel to the heliospheric field (Swisdak et al. 2010). In Swisdak et al. we assumed that the heliosheath field was laminar with an organized polarity in each hemisphere. What happens when a laminar interstellar magnetic field approaches a sea of magnetic islands needs to be investigated.

The sector region is carried to the north so *Voyager 1* is expected to remain inside the sector region all the way to the HP. *Voyager 2*, after leaving the sector region in 2009.15, is expected to eventually re-enter the sector region, but at a radial location much closer to the HP.

In this work we focused mainly on the energetic electrons. However, we expect that because of the north–south asymmetry of the sector region there will be an asymmetry in the intensity of the ACRs between *Voyager 2* in the southern hemisphere and *Voyager 1* in the northern hemisphere. This should be more visible as the HCS moves to lower latitudes than *Voyager 2*. Current analysis of the data does not reveal the spatial intensity gradients because the ACRs are dominated by temporal variations (Decker et al. 2009). Future studies will have to disentangle the temporal variation in order to confirm our prediction of a gradient between *Voyager 1* and *2*.

M.O. acknowledges the support of NASA-*Voyager* Guest Investigator Grant NNX07AH20G. This work is also supported by the National Science Foundation CAREER Grant ATM-0747654. J.D. and M.S. were supported by grant ATM-0903964. M.O. especially thanks the staff of the NASA Supercomputer Division at Ames and the Pleiades award SMD-10-1600 that allowed the simulations to be performed. The PIC simulations were carried out at the National Energy Research Super Computer Center. Work at JHU/APL was supported by the NASA *Voyager* Interstellar Mission, Contact NNX07AB02G. We acknowledge the fruitful discussions with M.E. Hill. This research benefited greatly from discussions that were held at the meetings of the International Team devoted to understanding the suprathermal ion tails and ACRs that has been sponsored by the International Space Science Institute in Bern, Switzerland.

REFERENCES

Alexashov, D., & Izmodenov, V. V. 2005, A&A, 439, 1171
Borovikov, S. N., Pogorelov, N. Y., Burlaga, L. F., & Richardson, J. D. 2011, ApJ, 728, L21
Burlaga, L. F., & Ness, N. F. 1968, Can. J. Phys., 46, 1962
Burlaga, L. F., Ness, N. F., & Richarson, J. D. 2003, J. Geophys. Res., 108, 8028
Burlaga, L. F., & Ness, N. F. 2009, ApJ, 703, 311
Burlaga, L. F., Ness, N. F., Acuna, M. H., Wang, Y.-M., & Sheeley, N. R., Jr. 2009, J. Geophys. Res., 114, A06106
Burlaga, L. F., & Ness, N. F. 2010, ApJ, 725, 1306
Burlaga, L. F., Ness, N. F., Wang, Y. -M., Sheeley, N. R., & Richardson, J. D. 2010, J. Geophys. Res., 115, A08107
Czechowski, A., Strumik, M., Grygorczuk, J., Grzedzielski, S., Ratkiewicz, R., & Scherer, K. 2010, A&A, 516, A17
Decker, R. B., Krimigis, S. M., Roelof, E. C., & Hill, M. E. 2010, in AIP Conf. Proc. 1302, Pickup Ions throughout the Heliosphere and Beyond: 9th Ann. Int. Astrophysics Conf., ed. J. le Roux et al. (Melville, NY: AIP), 51
Drake, J. F., Opher, M., Swisdak, M., & Chamoun, J. N. 2010, ApJ, 709, 963
Drake, J. F., Swisdak, M., Che, H., & Shay, M. A. 2006, Nature, 443, 553
Fisk, L. A., & Gloeckler, G. 2006, ApJ, 640, L79
Fisk, L. A., & Gloeckler, G. 2007, in Proc. of National Academy of Sciences, 104, 5749
Fisk, L. A., & Gloeckler, G. 2009, Advances in Space Research, 43, 1471
Heerikhuisen, J., et al. 2010, ApJ, 708, L126
Izmodenov, V. V. 2009, Space Sci. Rev., 143, 139
Lazarian, A., & Opher, M. 2009, ApJ, 703, 8
McComas, D. J., & Schwadron, N. A. 2006, Geophys. Res. Lett., 33, L04102
McComas, D. J., et al. 2009, Science, 326, 959
Opher, M., Alouani Bibi, F., Toth, G., Richardson, J. D., Izmodenov, V. V., & Gombosi, T. I. 2009, Nature, 462, 1036
Opher, M., Stone, E. C., & Gombosi, T. I. 2007, Science, 316, 875
Opher, M., Stone, E. C., & Liewer, P. C. 2006, ApJ, 640, L71
Pogorelov, N. V., Heerikhuisen, J., & Zank, G. 2008, ApJ, 675, L41
Pogorelov, N. V., et al. 2007, in AIP Conf. Ser. 932, Turbulence and Nonlinear Processes in Astrophysical Plasmas: 6th Annual International Astrophysics Conference, ed. D. Shaikh & G. P. Zank (Melville, NY: AIP), 129
Ratkiewicz, R., & Grygorczuk, J. 2008, Geophys. Res. Lett., 35, L23105
Richardson, J. D., Kasper, J. C., Wang, C., Belcher, J. W., & Lazarus, A. J. 2008, Nature, 454, 63
Smith, E. J. 2001, J. Geophys. Res., 106, 15819
Stone, E. C., Cummings, A. C., McDonald, F. B., Heikkila, B. C., Lal, N., & Webber, W. R. 2005, Science, 309, 2017
Stone, E. C., Cummings, A. C., McDonald, F. B., Heikkila, B. C., Lal, N., & Webber, W. R. 2008, Nature, 454, 71
Swisdak, M., Opher, M., Drake, J., & Alouani-Bibi, F. 2010, ApJ, 710, 1769
Toth, G., et al. 2011, J. Comput. Phys, in press
Zank, G. P. 1999, Space Sci. Rev., 89, 413
Zank, G. P., Pauls, H. L., Williams, L. L., & Hall, D. T. 1996, J. Geophys. Res., 101, 21639
Zeiler, A., Biskamp, D., Drake, J. F., Rogers, B. N., Shay, M. A., & Scholer, M. 2002, J. Geophys. Res., 107, 1230